

Correlation of JMA instrumental seismic intensity with strong motion parameters

Kazi R. Karim^{*,†} and Fumio Yamazaki

Institute of Industrial Science, University of Tokyo, Tokyo 153-8505, Japan

SUMMARY

The Japan Meteorological Agency (JMA) seismic intensity (I_{JMA}) has been used as a measure of strong shaking for many years in Japan, and it necessitates to know the correlation between the JMA seismic intensity and other strong motion indices, e.g. Peak Ground Acceleration (PGA), Peak Ground Velocity (PGV), and Spectrum Intensity (SI). In this study, two strong motion data sets were selected; in which, the first set consists of 879 three-components non-liquefied records selected from 13 major earthquake events that occurred in Japan, the United States, and Taiwan, and the second set consists of 17 liquefied records selected from 7 major earthquake events that occurred in Japan and the United States. The JMA seismic intensity and other ground motion indices were calculated using the selected data sets. The relationships between the JMA seismic intensity and PGA, PGV, and SI were then derived performing a two-stage linear regression analysis. Results from the analysis show that the JMA instrumental seismic intensity shows higher correlation with SI than PGA or PGV, and it shows the highest correlation with the parameters such as the combination of PGA and SI or the product of PGA and SI. The obtained relationships are also compared with the ones obtained by other studies, which may be useful for the disaster management agencies in Japan and deployment of new SI-sensors that monitor both PGA and SI. Copyright © 2002 John Wiley & Sons, Ltd.

KEY WORDS: JMA seismic intensity; seismometer; SI-sensor; strong motion records; ground motion indices; regression analysis

1. INTRODUCTION

The Japan Meteorological Agency (JMA) seismic intensity (I_{JMA}) has been used as a measure of strong shaking for many years in Japan. It was determined by the human judgment of JMA officers. However, in the early 1990s, the JMA started to move towards an instrumental seismic intensity (Figure 1) rather than human judgment. In 1996, the JMA intensity scale [1] was revised and a large number of seismometers (574 in total) measuring the JMA intensity were deployed throughout Japan [2]. In this objective, Shabestari and Yamazaki [3]

* Correspondence to: Kazi R. Karim, Yamazaki Laboratory, Institute of Industrial Science, the University of Tokyo, 4-6-1 Komaba, Meguro-ku, Tokyo 153-8305, Japan.

† E-mail: kazi@rattle.iis.u-tokyo.ac.jp

Received 20 April 2001

Revised 1 August 2001

Accepted 22 October 2001

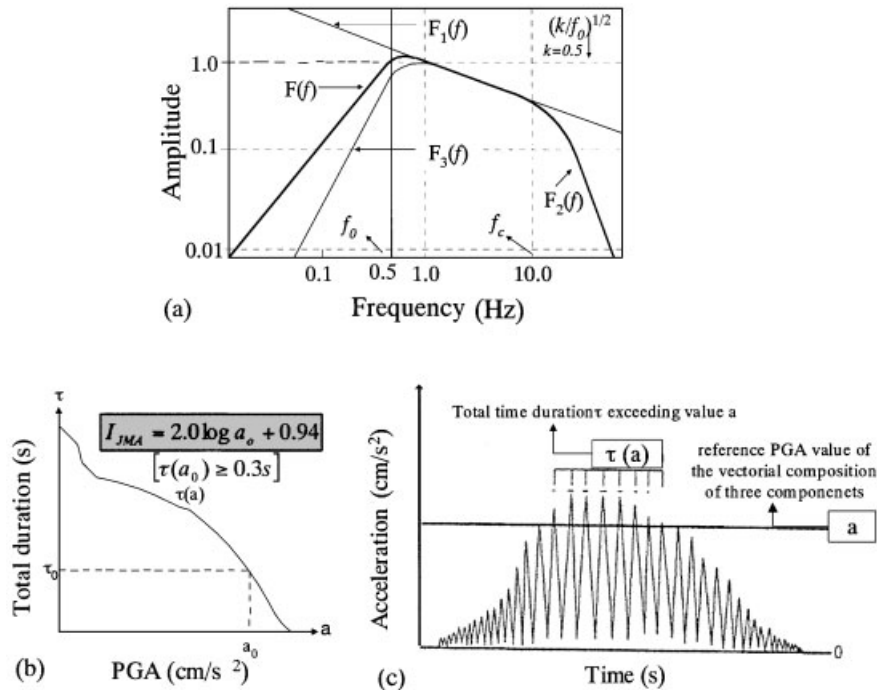


Figure 1. Calculation of JMA instrumental seismic intensity, which is obtained (a) applying a band pass filter in the frequency domain and (b) considering the durational effect $\tau(a)$ of PGA, which is obtained in the time domain by (c) summing the time segments exceeding a reference PGA value of the vectorial composition of the three-components of acceleration records.

developed an attenuation relationship of JMA seismic intensity using JMA records. Recently, the Fire and Disaster Management Agency (FDMA) also deployed one seismometer measuring JMA intensity in each municipality (3255 in total). Using these networks, the distribution of intensity due to an earthquake can be estimated even in the case of a very localized event. The disaster management agencies in Japan use the JMA intensity as the most important index for estimating structural damage, identifying affected areas, and preparing for crisis management due to earthquakes [4, 5].

Other ground motion indices, e.g., Peak Ground Acceleration (PGA), Peak Ground Velocity (PGV), Spectrum Intensity (SI), etc., are also used to describe the severity of an earthquake. Tong and Yamazaki [6] investigated the relationship between ground motion severity and house damage ratio based on the house damage data selected from major earthquakes in Japan including the 1995 Hyogoken–Nanbu (Kobe) earthquake. They concluded that SI has the higher correlation with house damage ratio than other ground motion indices. In Japan, the SI value (Figure 2) is used as the index to shut-off the natural gas supply after a damaging earthquake. Based on the seismic records and damage of gas pipes around the instruments due to the 1995 Kobe earthquake, a SI value of 60 cm/s was set as the level of shaking for mandatory shut-off a city gas supply. In this objective, Tokyo Gas Co. Ltd has developed an SI-sensor [7] and a new SI-sensor [8], which calculate the SI value in the sensor using

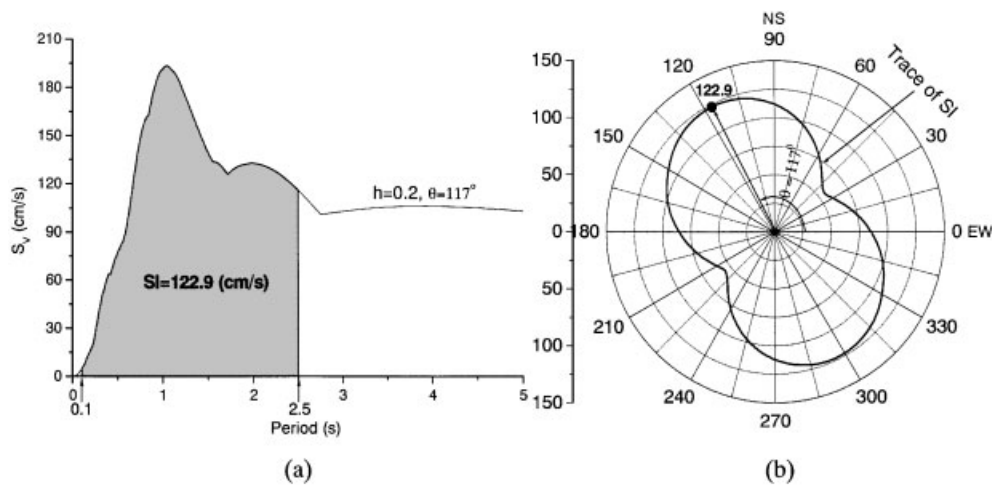


Figure 2. (a) Definition of Spectrum Intensity (SI), which is calculated as the area under the relative-velocity response spectrum with 20% damping ratio between the periods of 0.1 s and 2.5 s, divided by the period interval, and (b) trace of SI, which is computed from the EW and NS components of acceleration records of the JMA Kobe station of the 1995 Kobe earthquake. The maximum value of SI is shown on the trace with a solid circle, which is obtained at $\theta = 117^\circ$.

horizontal acceleration records. Recently, the deployment of new SI-sensors has started in the Tokyo metropolitan area, and the Super Dense Seismic Monitoring System-‘SUPREME’ [9, 10] with 3700 new SI-sensors will be completed by the year 2007. Note that in Taiwan, 31 new SI-sensors have been installed in an 80km² area in the Taipei city by the Great Taipei Gas Co. Ltd, and Shimizu *et al.* [11] studied the site amplification factor of main shock of the 1999 Chi-Chi earthquake based on the seismic motion observed in Taipei basin by new SI-sensors. They found that the site amplification of the main shock can be estimated by the site amplification of aftershocks. In other words, the seismic motion measurement in a small earthquake is quite important for seismic zonation.

Hence, it is important to know the relationship between the new JMA instrumental seismic intensity and other strong motion indices (e.g., PGA, PGV, and SI). Midorikawa [12], Midorikawa and Fukuoka [13], and Midorikawa *et al.* [14] investigated the correlation between the JMA seismic intensity and physical parameters of earthquake ground motion. They also investigated the correlation between the new JMA instrumental seismic intensity and the former JMA seismic intensity. Tong and Yamazaki [15] also obtained the relationship between ground motion indices and JMA instrumental seismic intensity. However, the correlation between seismic intensity and ground motion indices might differ depending upon the selection criteria of the records, number of records used, distribution of ground motion indices, and the method of analysis. The earthquake records used by Midorikawa *et al.* [12–14] were recorded mostly by SMAC-B2 type accelerometers, which requires instrumental correction. The ground motion records used by Tong and Yamazaki [15] were both JMA and non-JMA records from recent earthquakes in Japan and the United States. They used 205 selected records to give wide variability in intensity; however, the selected data may be expanded to cover a wider variation in spectral intensity and durational characteristics of seismic records.

In this study, two strong motion data sets are selected; in which, the first set consists of 879 three-components non-liquefied acceleration records selected from 13 major earthquake events that occurred in Japan, the United States, and Taiwan. These events are selected to cover the magnitude (M_W) range between 5 to 8. All the free-field records having a PGA greater than or equal to 10 cm/s^2 in one of the horizontal components were selected in the first data set. The second data set consists of 17 three-components liquefied acceleration records [16, 17] selected from seven earthquake events that occurred in Japan and the United States. The new JMA seismic intensity and other ground motion indices are calculated using the selected data sets. The relationships between JMA intensity and PGA, PGV and SI are then derived performing a two-stage linear regression analysis. The new relationships are compared with the ones obtained by other studies [12–15], which may be useful for the disaster management agencies in Japan and deployment of new SI-sensors that monitor both PGA and SI.

STRONG MOTION PARAMETERS

JMA seismic intensity

The JMA seismic intensity scale was revised recently [1]. First, the Fourier transform (FT) is applied for the selected time window for the three components of acceleration time histories. Then, a band-pass filter equation (1) is applied in the frequency domain as shown in Figure 1(a):

$$F(f) = F_1(f)F_2(f)F_3(f) \quad (1)$$

in which

Period-effect filter:

$$F_1(f) = \sqrt{1/f} \quad (2)$$

High-cut filter:

$$F_2(f) = \frac{1}{\sqrt{1 + 0.694x^2 + 0.241x^4 + 0.0557x^6 + 0.009664x^8 + 0.00134x^{10} + 0.000155x^{12}}} \quad (3)$$

$(x = \sqrt{1/f_c})$

Low-cut filter:

$$F_3(f) = \sqrt{1 - \exp(-f/f_0)^3} \quad (4)$$

where f is the frequency of the ground motion, f_c is the reference frequency for high-cut filter, and f_0 is the reference frequency for low-cut filter. After taking the Inverse Fourier Transform (IFT), the effect of the duration (τ) was considered for a vectorial composition of the three-components that is made in the time domain (Figure 1(b)). Considering an acceleration value a_0 having total duration τ satisfying the condition $\tau(a_0) \geq 0.3 \text{ s}$ (Figure 1(c)), the JMA seismic intensity (I_{JMA}) is calculated by using Equation (5) as a real (continuous) number

$$I_{\text{JMA}} = 2.0 \log a_0 + 0.94 \quad (5)$$

PGA and PGV

The Peak Ground Acceleration (PGA) and Peak Ground Velocity (PGV) are defined as the maximum of the resultant of the two horizontal components in the directions as originally recorded and denoted by PGA_R and PGV_R .

Spectrum intensity

The Spectrum Intensity (SI) is calculated as the area under the relative-velocity response spectrum with 20% damping ratio between the periods of 0.1 s and 2.5 s, divided by the period interval (Figure 2(a)), and it is defined as

$$SI = \frac{1}{2.4} \int_{0.1}^{2.5} S_v(T, h = 0.2) dT \quad (6)$$

where SI is the spectrum intensity, S_v is the relative-velocity response spectrum, T is the period, h is the damping ratio taken as 20%, and dT is the period interval taken as 0.1s. Several definitions exist for calculating SI, e.g., SI can be larger of the two horizontal components or it can be obtained from either of the definition of the Ministry of Construction, Japan or Tokyo Gas Co. Ltd. According to the Ministry of Construction, SI is computed from the vectorial composition of the two horizontal velocity responses, and according to the Tokyo Gas Co. Ltd, it is computed as rotating the two horizontal components (EW and NS) of acceleration records from 0 to 180° with 1° interval on the horizontal plane and the maximum SI is considered as the SI value. In this study, SI is calculated according to this definition. Figure 2(b) shows the trace of SI, which is computed from the EW and NS components of acceleration records of the JMA Kobe station of the 1995 Kobe earthquake by rotating the two horizontal components of acceleration records from 0 to 180° with 1° interval. One can see that the maximum value of SI is 122.9 cm/s, which is shown on the trace (Figure 2(b)) with a solid circle. Hence, according to the Tokyo Gas Co. Ltd definition, the value of SI should be considered as 122.9 cm/s.

EARTHQUAKE DATA

Two earthquake data sets are used in this study. The first data set consists of 879 three-components non-liquefied acceleration records selected from 13 major earthquake events that occurred mostly in Japan, two in the United States, and one in Taiwan, and the magnitude (M_W) for the selected earthquake events ranges from 5.4 to 8.3. The second data set consists of 17 three-components liquefied acceleration records selected from seven major earthquake events that occurred mostly in Japan and one in the United States, and the magnitude (M_W) for the selected events ranges from 6.0 to 8.2. Hereafter, we call the first data set as non-liquefied records and the second data set as liquefied records. The two data sets of the strong motion records are limited to

1. Acceleration records only from free-field sites were selected.
2. Acceleration records with a PGA greater than or equal to 10cm/s^2 in one of the horizontal components were included in the data set.

3. The acceleration records include both far- and near-field ones.
4. In case of closely located stations, only one record was selected and others were omitted.
5. Records from the liquefied and liquefaction-suspicious sites were selected according to the following classification [17]:
 - (a) *Liquefied sites*: There was evidence seen for liquefaction at the recording site.
 - (b) *Liquefaction-suspicious sites*: There was no evidence seen for liquefaction at the recording site, but it was observed in its vicinity (up to 50 m) or cyclic mobility at the site was confirmed by an analytical study.
 - (c) *Non-liquefied sites*: There was no evidence for liquefaction at the recording site and its vicinity (up to 50 m) as well as no confirmation about the cyclic mobility at the site.

The American records were obtained from the Earthquake Strong Motion CD-ROM, National Geographic Data Center [18] and from the Internet site of California Strong Motion Instrumentation Program (CSMIP). The Taiwanese records were retrieved from the CD-ROM of free-field strong ground motion data, Seismological Center of the Central Weather Bureau [19]. The Japanese records were provided by many national organizations, institutes and private companies including Japan Meteorological Agency (JMA), Port and Harbor Research Institute (PHRI), Ministry of Transport, Public Works Research Institute (PWRI), Ministry of Construction, Kyoshin-NET (K-NET), National Research Institute of Earth Science and Disaster Prevention, and Tokyo Gas Co. Ltd. The summary of the non-liquefied and liquefied records used in this study is shown in Tables I and II, respectively. Figure 3(a) shows the distribution of magnitude and JMA intensity for the 879 non-liquefied records used in this study and the distribution of magnitude and PGA_R is shown in Figure 3(b). The distribution of PGA_R and SI, and PGV_R and SI are shown in Figures 3(c) and 3(d), respectively. Note that some of the largest intensities calculated for the all records of the non-liquefied data are

Table I. Summary of the earthquake records (non-liquefied) used in this study and the regression coefficients obtained for each earthquake event with respect to SI.

No.	Earthquake event	Event date	M_W^*	No. of records	Regression coefficients for SI			
					b_0	b_1	σ	R^2
1	Chibaken-Toho-Okai	17/12/87	6.5	22	2.38	1.97	0.096	0.965
2	Loma Prieta	17/10/89	6.9	54	2.26	1.96	0.131	0.953
3	Kushiro-Okai	15/01/93	7.6	36	2.48	1.95	0.225	0.959
4	Hokkaido-Nansei-Okai	12/07/93	7.7	5	2.21	2.04	0.214	0.959
5	Northridge	17/01/94	6.7	44	2.53	1.82	0.105	0.976
6	Hokkaido-Toho-Okai	04/10/94	8.3	18	2.42	2.00	0.182	0.963
7	Sanriku-Haruka-Okai	28/12/94	7.7	6	2.28	2.05	0.246	0.951
8	Kobe	17/01/95	6.9	34	2.25	1.98	0.124	0.989
9	Kagoshima-Hokusei	26/03/97	6.1	67	2.43	1.88	0.182	0.959
10	Kagoshima-Hokusei	13/05/97	6.1	63	2.40	1.93	0.149	0.975
11	Izu Peninsula	03/05/98	5.5	22	2.46	1.90	0.099	0.984
12	Tokyo Bay	29/08/98	5.4	89	2.52	1.80	0.171	0.927
13	Chi-Chi	20/09/99	7.7	419	2.23	1.94	0.112	0.971

* Moment magnitude provided by Harvard University.

Table II. Summary of the earthquake records (liquefied) used in this study.

No.	Earthquake event	Event date	M_W^*	No. of records
1	Niigata	16/06/64	7.6 [†]	1
2	Tokachi-Oki	16/05/68	8.2	1
3	Nihonkai Chubu	26/05/83	7.7	1
4	Superstition Hills	24/11/87	6.0	1
5	Loma Prieta	18/10/89	6.9	1
6	Kushiro-Oki	15/01/93	7.6	1
7	Kobe	17/01/95	6.9	11

* Moment magnitude provided by Harvard University.

† Moment magnitude provided by Aki [30].

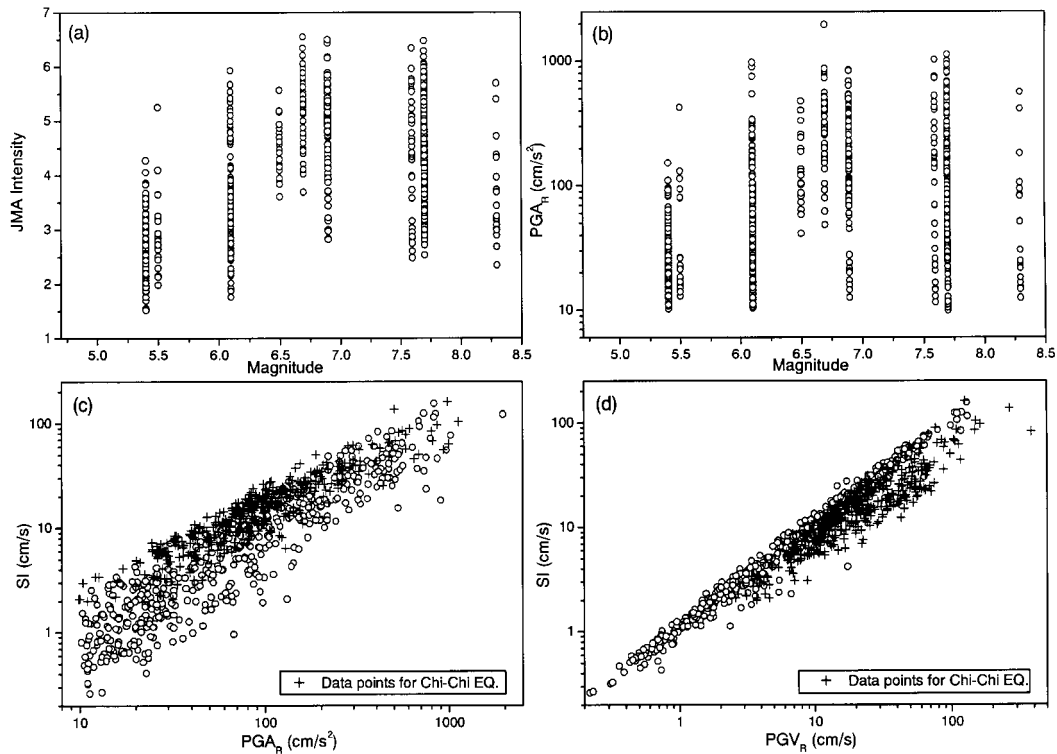


Figure 3. Distribution of (a) magnitude and JMA intensity, (b) magnitude and PGA_R , (c) PGA_R and SI, and (d) PGV_R and SI for the 879 non-liquefied records used in this study.

6.44 for the JMA Kobe station of the Kobe earthquake, 6.48 for the TCU084 station of the Chi-Chi earthquake, and 6.55 for the Tarzana station of the Northridge earthquake. Figure 4(a) shows the distribution of PGA_R and SI for the 17 liquefied records used in this study and the distribution of PGV_R and SI is shown in Figure 4(b). The linear relationship between

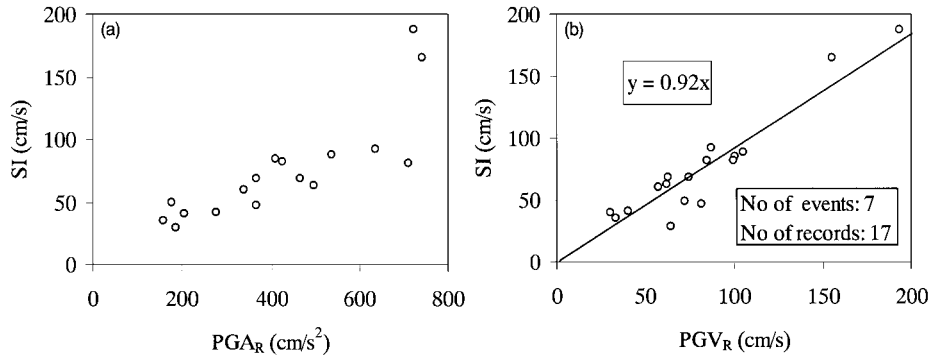


Figure 4. (a) Distribution of PGA_R and SI, and (b) relationship between PGV_R and SI for the 17 liquefied records used in this study.

PGV_R and SI (Figure 4(b)) for the liquefied records is different from the one obtained for non-liquefied records [6].

REGRESSION MODEL

The regression model used in this study is given as

$$y = b_0 + b_1M + b_2 \log_{10} x_1 \quad (\text{Univariate}) \quad (7)$$

$$y = b_0 + b_1M + b_2 \log_{10} x_1 + b_3 \log_{10} x_2 \quad (\text{Multivariate}) \quad (8)$$

where y is the JMA instrumental seismic intensity (I_{JMA}), b_0 , b_1 , b_2 , and b_3 are the regression coefficients, M is the magnitude, and x_1 and x_2 are the ground motion indices, i.e., PGA, PGV and SI. The regression models given in Equations (7) and (8) are linear with respect to the coefficients to be determined. However, the correlation between magnitude and ground motion indices might result in systematic error if simple linear regression is used [20]. Choice in deriving prediction equations involves the details of how the data are to be used in determining the unknown coefficients [21]. In this case, a potential for bias exists for two reasons: first, the data are not uniformly distributed and they may be dominated by many recordings from a few earthquakes [22]. They concluded that a two-stage regression method, introduced by Joyner and Boore [23] to separate one variable dependence from another variable dependence, is desirable. For instance, in the regression model equation (7), one can see that there are two variables, one is the magnitude and the other one is the ground motion indices. Hence, in this case, it is desirable that we should separate the ground motion indices dependence from magnitude dependence. The advantage of the two-stage linear regression analysis is to let each recording have equal weight in determining the shape, and each earthquake have equal weight in determining the magnitude scaling [22]. Hence, in this study, a two-stage linear regression analysis is performed for deriving the relationship between JMA seismic intensity and other ground motion indices.

If the two-stage regression was applied to Equation (7), then the first stage is the least-squares regression of

$$y = \sum_{j=1}^k a_j A_j + b_2 \log_{10} x_1 \quad (9)$$

where k is the number of earthquakes, and $A_j = 1$ for earthquake j ; $A_j = 0$ otherwise. The second stage is the weighted least-squares regression of

$$a_j = b_0 + b_1 M_j \quad (10)$$

where a_j is determined in the first stage and known as the offset factors, which are used in order to let each earthquake event have equal weight. Equation (9) can be represented by [24–26]

$$Y = X\beta + \varepsilon \quad (11)$$

where

$$X = \begin{bmatrix} A_{1,1} & A_{2,1} & \dots & A_{k,1} & \log_{10} x_1 \\ A_{1,2} & A_{2,2} & \dots & A_{k,2} & \log_{10} x_2 \\ \vdots & \vdots & & \vdots & \vdots \\ A_{1,n} & A_{2,n} & \dots & A_{k,n} & \log_{10} x_n \end{bmatrix} \quad (12)$$

and β and ε are the regression coefficient and residual vectors, respectively. One should note that in Equations (7) and (8), x_1 and x_2 represent two independent variables, say, PGA and PGV, on the other hand, in Equation (12), x_1 , x_2 , and x_n represent the number of observations of a particular independent variable, for instance, the number of PGA for the non-liquefied records is 879. The least-squares solution of Equation (11) is

$$b = (X^T X)^{-1} X^T Y \quad (13)$$

where b is the estimator of β , and the expected value $E(b)$ is β . Note that in case of multivariate analysis, the procedure remains the same with a little change of the X matrix in Equation (12). In this case, the values of the additional independent variable should be entered in the X matrix in the form of adding one more column to the right of the first independent variable column.

Figure 5(a) shows the plots of slope b (coefficient of SI) vs. magnitude of each earthquake event obtained for the non-liquefied records and the regression coefficients obtained for individual event with respect to SI are given in Table I. Figure 5(b) shows the plots of offset factor a_j vs magnitude of each earthquake event, which is obtained in the first stage. In the second-stage regression analysis, the offset factors are used in order to let each event have equal weight in determining the magnitude scaling, and the relationships between JMA intensity and SI obtained for different magnitudes are shown in Figure 5(c). Figure 5(d) shows the relationships between JMA intensity and SI obtained from simple and two-stage linear regression analyses. The relationships obtained for the all earthquake events and the relationship

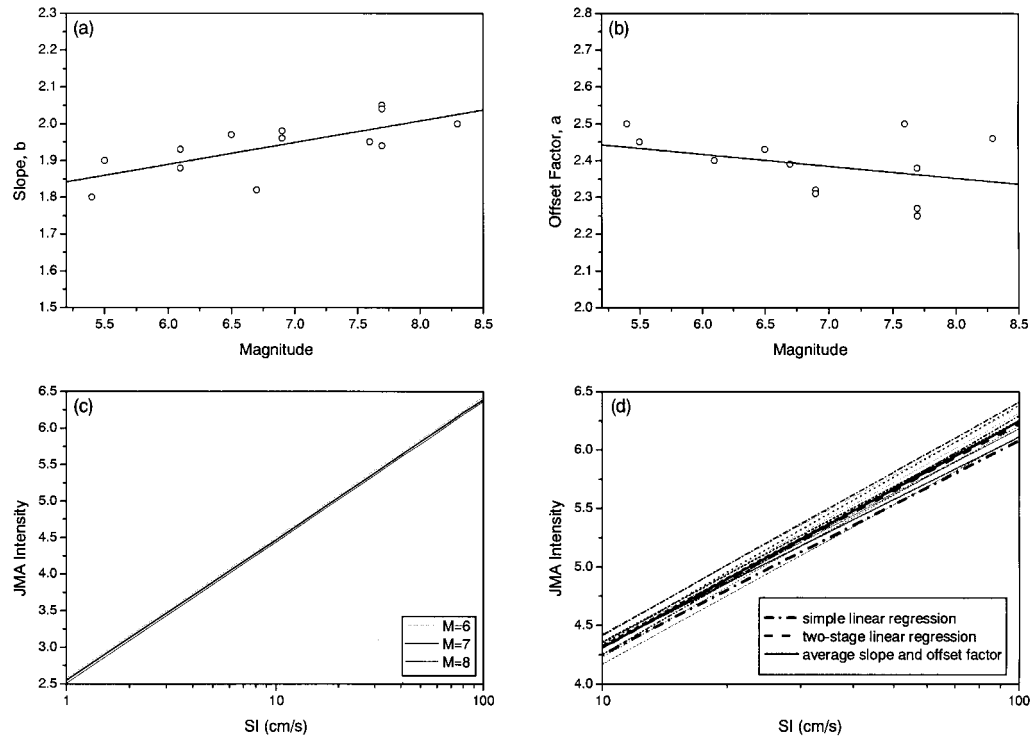


Figure 5. (a) Slope b (coefficient of SI) of individual event with respect to magnitude, (b) offset factor a_j of individual event with respect to magnitude, which is used to let each earthquake event have equal weight, (c) relationship between JMA intensity and SI for different magnitudes, and (d) comparison of the relationships between JMA intensity and SI obtained from simple and two-stage linear regression analyses. The relationships obtained for the all earthquake events and the relationships obtained from the average slope and offset factor of the all events are also shown in the same figure. All the plots shown in the figure are based on the non-liquefied records.

obtained from the average slope and offset factor of the all events are also shown in Figure 5(d). The slopes obtained from simple and two-stage linear regression analyses are 1.83 and 1.92, respectively, and the average slope for the all earthquake events is 1.94. It means that the average slope of the all events and the slope obtained from two-stage linear regression analysis are very close to each other, on the other hand, the slope obtained from simple linear regression analysis shows a lower value comparing to the one obtained from two-stage linear regression analysis. One can see (Figure 5(d)) that the relationship between the JMA seismic intensity and SI obtained from two-stage linear regression analysis is very similar comparing to the one obtained from the average slope and offset factor of the all events. One can also see (Figure 5(d)) that the relationships between JMA intensity and SI obtained from two-stage linear regression analysis and obtained from the average slope and offset factor of the all events pass almost through the mid-point of the relationships of the all events, however, the relationship obtained from simple linear regression analysis shows a lower value for the

higher value of SI comparing to the other relationships. Moreover, the correlation coefficient obtained from two-stage linear regression analysis ($R^2 = 0.982$) is higher comparing to the one obtained from simple linear regression analysis ($R^2 = 0.975$). It implies that in case of many earthquake events, if we perform simple linear regression analysis, then there is a possibility that we may underestimate (or sometimes overestimate) the JMA seismic intensity from strong motion parameters. In order to avoid this problem, all the regression results are obtained in this study based on the two-stage linear regression analysis.

RESULTS AND DISCUSSIONS

Results obtained from non-liquefied records

The linear relationships between JMA intensity and ground motion indices for the non-liquefied records are derived in this study as

$$I_{\text{JMA}} = -0.65 + 0.18M + 1.81 \log_{10} \text{PGA}_{\text{R}} \quad (\sigma = 0.302, R^2 = 0.942) \quad (14)$$

$$I_{\text{JMA}} = 3.35 - 0.13M + 1.82 \log_{10} \text{PGV}_{\text{R}} \quad (\sigma = 0.345, R^2 = 0.937) \quad (15)$$

$$I_{\text{JMA}} = 2.61 - 0.03M + 1.92 \log_{10} \text{SI} \quad (\sigma = 0.160, R^2 = 0.982) \quad (16)$$

The relationships are also derived using other parameters, such as, the product of two ground motion indices or the combination of two ground motion indices. In this case, the relationships are derived as

$$I_{\text{JMA}} = 1.33 + 0.01M + 0.98 \log_{10}(\text{PGA}_{\text{R}} \text{PGV}_{\text{R}}) \quad (\sigma = 0.203, R^2 = 0.975) \quad (17)$$

$$I_{\text{JMA}} = 0.89 + 0.07M + 0.98 \log_{10}(\text{PGA}_{\text{R}} \text{SI}) \quad (\sigma = 0.126, R^2 = 0.987) \quad (18)$$

$$I_{\text{JMA}} = 1.58 + 0.02M + 1.38 \log_{10} \text{SI} + 0.59 \log_{10} \text{PGA}_{\text{R}} \quad (\sigma = 0.104, R^2 = 0.991) \quad (19)$$

$$I_{\text{JMA}} = 1.27 + 0.01M + 0.95 \log_{10} \text{PGV}_{\text{R}} + 1.00 \log_{10} \text{PGA}_{\text{R}} \quad (\sigma = 0.202, R^2 = 0.975) \quad (20)$$

where I_{JMA} is the JMA intensity, M is the magnitude (M_{W}), PGA_{R} and PGV_{R} are the resultant of the two horizontal components, SI is the maximum of SI calculated from 0 to 180° in the horizontal plane with 1° interval, σ is the standard deviation, and R is the correlation coefficient.

Table III shows the list of the regression coefficients obtained for the non-liquefied records in this study and by other studies [14, 15]. Figure 5(c) shows the relationship between JMA intensity and SI for a magnitude of 6–8. One can see that the relationships seem to be similar for different magnitudes. However, for a comparison with other studies, the relationships from Equations (14)–(20) are normalized for a magnitude of 7, and the new relationship takes into

Table III. List of the regression coefficients for the non-liquefied records obtained in this study and by other studies [14, 15].

Parameters (x_1, x_2)	$I_{JMA} = b_0 + b_1 M + b_2 \log_{10} x_1$ $I_{JMA} = b_0 + b_1 M + b_2 \log_{10} x_1 + b_3 \log_{10} x_2$										(Univariate) (Multivariate)					
	This study*					Midorikawa <i>et al.</i>					Tong and Yamazaki†					
	b_0	b_1	b_2	b_3	σ	R^2	b_0	b_1	b_2	b_3	σ	b_0	b_1	b_2	b_3	σ
PGAR	-0.65	0.18	1.81	—	0.302	0.942	0.55	—	1.90	—	0.30	0.59	—	1.89	—	0.281
PGVR	3.35	-0.13	1.82	—	0.345	0.937	2.68	—	1.72	—	0.21	2.30	—	2.01	—	0.418
SI	2.61	-0.03	1.92	—	0.160	0.982	—	—	—	—	—	2.34	—	1.96	—	0.174
PGAR PGVR	1.33	0.01	0.98	—	0.203	0.975	1.25	—	1.02	—	0.15	—	—	—	—	—
PGAR SI	0.89	0.07	0.98	—	0.126	0.987	—	—	—	—	—	—	—	—	—	—
PGAR, PGVR	1.27	0.01	1.00	0.95	0.202	0.975	2.57	—	0.35	—	0.95	1.11	—	1.25	0.78	0.180
PGAR, SI	1.58	0.02	0.59	1.38	0.104	0.991	—	—	—	—	—	1.68	—	0.69	1.29	0.097

* To compare with other studies, the regression equations are normalized for a magnitude of 7, and the normalized regression coefficients are shown in Table IV.

† The regression coefficients were obtained based on the larger of the two horizontal components of the earthquake records. To compare the results with this study, the regression equations were converted from larger to resultant of the two horizontal components using Table V, and the converted regression coefficients are shown in Table IV.

Table IV. Comparison of the regression coefficients for the non-liquefied records obtained in this study and by other studies [14, 15].

Parameters (x_1, x_2)	This study*			Midorikawa <i>et al.</i>			Tong and Yamazaki†		
	b_0	b_1	b_2	b_0	b_1	b_2	b_0	b_1	b_2
	$I_{JMA} = b_0 + b_1 \log_{10} x_1$ (Univariate)								
	$I_{JMA} = b_0 + b_1 \log_{10} x_1 + b_2 \log_{10} x_2$ (Multivariate)								
PGA _R	0.63	1.81	—	0.55	1.90	—	0.54	1.89	—
PGV _R	2.42	1.82	—	2.68	1.72	—	2.23	2.01	—
SI	2.39	1.92	—	—	—	—	2.30	1.96	—
PGA _R PGV _R	1.34	0.98	—	1.25	1.02	—	—	—	—
PGA _R SI	1.35	0.98	—	—	—	—	—	—	—
PGA _R , PGV _R	1.31	1.00	0.95	2.57	0.35	0.95	1.05	1.25	0.78
PGA _R , SI	1.74	0.59	1.38	—	—	—	1.64	0.69	1.29

* Normalized for a magnitude of 7.

† Converted from larger to resultant of the two horizontal components using Table V.

the following forms:

$$I_{JMA} = 0.63 + 1.81 \log_{10} \text{PGA}_R \quad (21)$$

$$I_{JMA} = 2.42 + 1.82 \log_{10} \text{PGV}_R \quad (22)$$

$$I_{JMA} = 2.39 + 1.92 \log_{10} \text{SI} \quad (23)$$

$$I_{JMA} = 1.34 + 0.98 \log_{10}(\text{PGA}_R \text{PGV}_R) \quad (24)$$

$$I_{JMA} = 1.35 + 0.98 \log_{10}(\text{PGA}_R \text{SI}) \quad (25)$$

$$I_{JMA} = 1.74 + 1.38 \log_{10} \text{SI} + 0.59 \log_{10} \text{PGA}_R \quad (26)$$

$$I_{JMA} = 1.31 + 0.95 \log_{10} \text{PGV}_R + 1.00 \log_{10} \text{PGA}_R \quad (27)$$

The normalized regression coefficients are listed in Table IV and the relationships (normalized for a magnitude of 7) of JMA intensity and ground motion indices obtained for the 879 non-liquefied records in this study are shown in Figures 6(a)–(c). It should be noted that the regression coefficients (Table III) obtained by Tong and Yamazaki [15] were based on the larger of the two horizontal components of the earthquake records (PGA_L, PGV_L, SI_L). To compare the results with this study, the regression equations of Tong and Yamazaki [15] were converted from larger to resultant of the two horizontal components using the mean ratio of larger/resultant (Figures 6(d)–(f)) obtained in this study, and the converted regression coefficients are shown in Table IV. The obtained mean ratios are very similar to the ones obtained in other studies [27, 28], and the comparison of the mean ratios is shown in Table V.

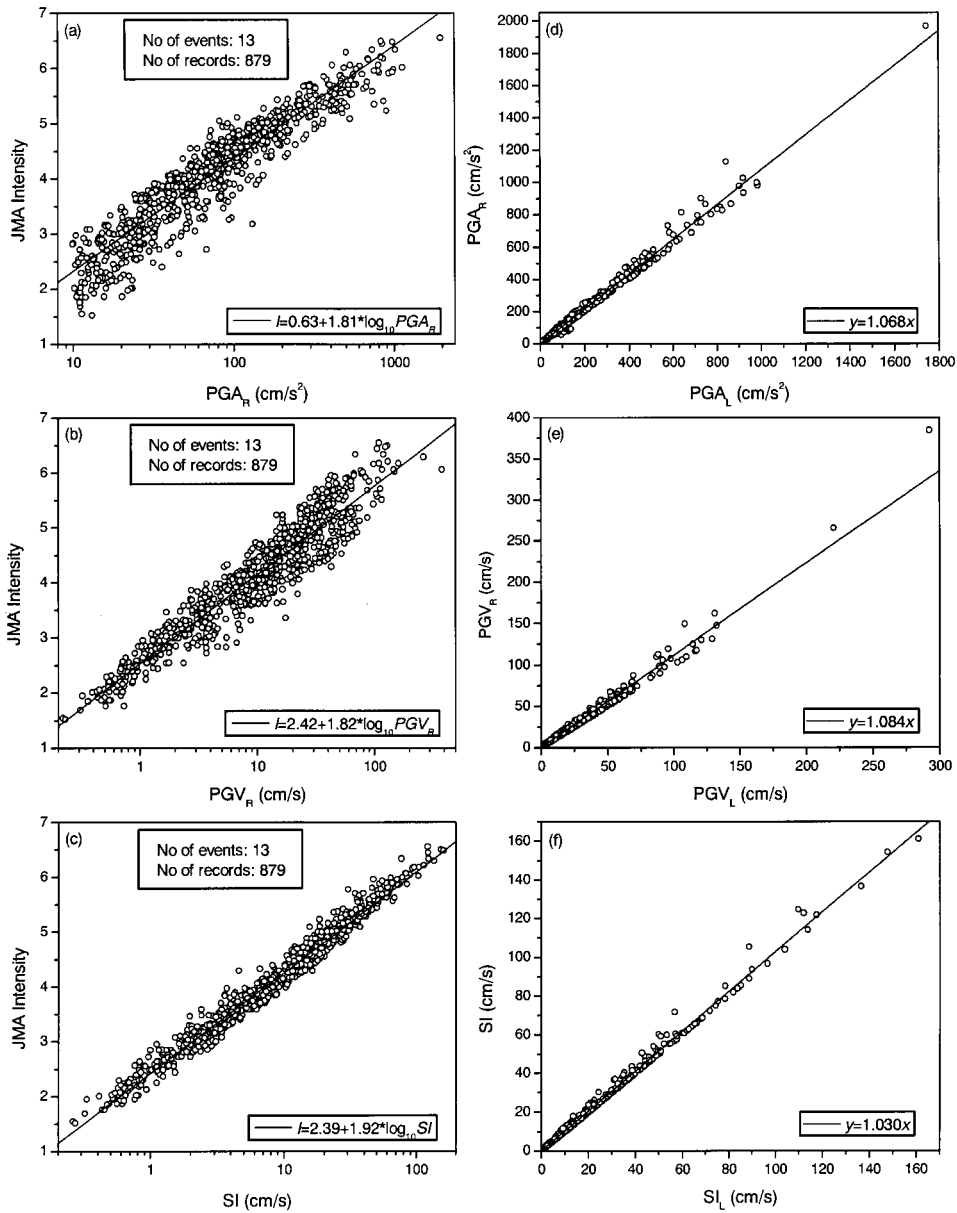


Figure 6. Relationships (normalized for a magnitude of 7) between (a) JMA intensity and PGA_R , (b) JMA intensity and PGV_R , and (c) JMA intensity and SI , and relationships between (d) PGA_L and PGA_R , (e) PGV_L and PGV_R , and (f) SI_L and SI obtained for the 879 non-liquefied records used in this study.

Table V. Comparison between the resultant/larger (for PGA and PGV) and max180/larger (for SI) ratios by this study and by other studies [27, 28].

Index	This study		Kawashima <i>et al.</i>		Ansary <i>et al.</i>	
	Mean	Std.	Mean	Std.	Mean	Std.
PGA	1.068	0.085	1.086	0.079	1.076	0.079
PGV	1.084	0.092	1.083	0.089	1.085	0.082
SI	1.030	0.055	—	—	—	—

Comparison of the results with other studies

Table IV shows the comparison of the normalized regression coefficients obtained in this study and the converted regression coefficients obtained by other studies [14, 15]. One can find some difference between the regression coefficients obtained in this study to the ones obtained in other studies. This difference comes might be due to the difference of the datasets and method of analysis. The data set used by Tong and Yamazaki [15] is well distributed and contains smaller values of intensity. On the other hand, the data set used in this study is well distributed, however, the range of JMA intensity is between 1.52 and 6.55. Again, the data set used by Midorikawa *et al.* [14] was recorded mostly by SMAC-B2 type accelerometers. Moreover, the conversion of the regression equations obtained by Tong and Yamazaki [15] was done based on the records used in this study, and not the actual records used by them.

Figure 7 shows the comparison of the relationships between I_{JMA} and PGA_R , PGV_R and SI, which are obtained in this study with the ones obtained in other studies [14, 15]. One can see that the relationship between JMA intensity and SI (Figure 7(c)) obtained in this study is very similar comparing to the one obtained by Tong and Yamazaki [15]. One can also see that the relationship between JMA intensity and PGA_R (Figure 7(a)) obtained in this study is very similar comparing to the ones obtained by Tong and Yamazaki [15] and Midorikawa *et al.* [14], however, some difference is observed with respect to PGV_R . The relationship between JMA intensity and PGV_R (Figure 7(b)) obtained in this study shows a little bit higher intensity value up to a PGV_R level of around 10 cm/s comparing to the one obtained by Tong and Yamazaki [15], and it shows a lower intensity value beyond that level, however, the same relationship shows a lower value comparing to the one obtained by Midorikawa *et al.* [14].

Figure 7(d) shows the plots of the residuals of I_{JMA} obtained from: (1) two-stage single variable linear regression analysis, and (2) two-stage multiple variables linear regression analysis. It can be seen that the linear fit of the residuals, in the case when I_{JMA} is estimated using both SI and PGA, is more or less close to the zero line. On the other hand, the linear fit of the residuals, in the case when I_{JMA} is estimated using only SI, has the tendency to be away from the zero line for higher values of I_{JMA} . This clearly indicates a better estimation of JMA intensity if both SI and PGA are considered rather than only SI. Figure 7(e) shows the relationship between the JMA intensity estimated in this study using SI and PGA and the JMA intensity estimated by Tong and Yamazaki [15]. It can be seen that the ratio of JMA intensity estimated in this study to the JMA intensity estimated by Tong and Yamazaki [15] is 1.00. It means, JMA intensity estimated for the two cases is the same. This good agreement

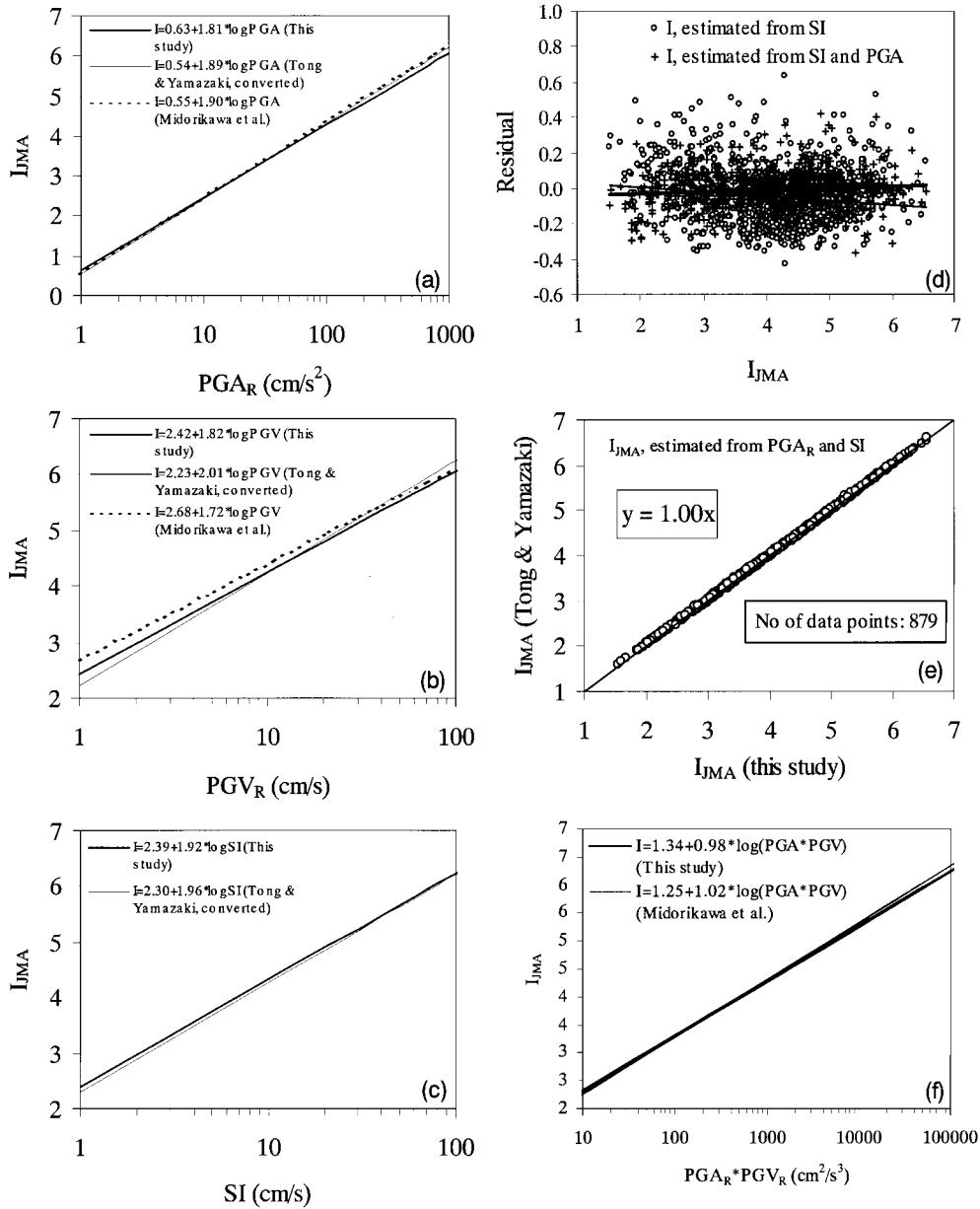


Figure 7. Comparison of the relationships between JMA intensity and ground motion indices (non-liquefied) obtained in this study with the ones obtained by other studies [14, 15]. The plots of the residuals of I_{JMA} obtained from single and multiple ground motion indices are also shown in (d) at the top right corner.

was also observed in case of single ground motion index SI (Figure 7(c)) that was explained earlier. The JMA intensity is also estimated using other parameters, such as, the product of two ground motion indices. Figure 7(f) shows the comparison of the relationship between JMA intensity and the product of PGA and PGV obtained in this study to the one obtained by Midorikawa *et al.* [14]. One can see that the relationships obtained in the both studies are very similar.

The correlation coefficients and as well as the standard deviations are also obtained while deriving the linear relationships between JMA intensity and all other parameters. The correlation coefficients obtained in this study are listed in Table III. It is observed that the correlation coefficient obtained for SI is higher than PGV or PGA. In case of the parameters such as the product of two ground motion indices, the correlation coefficient obtained for the product of PGA and SI is higher than the product of PGA and PGV. Similarly, for multivariate analysis, the correlation coefficient obtained for PGA and SI is higher than PGA and PGV. Midorikawa *et al.* [14] concluded that the instrumental seismic intensity shows higher correlation with PGV than PGA, and it shows the highest correlation with the parameters such as the product of PGA and PGV. However, in this study, it is observed that JMA intensity shows higher correlation with SI than PGA and PGV, and it shows the highest correlation with the parameters such as the combination of both PGA and SI or the product of PGA and SI. Note that the larger correlation coefficient in each category is shown in Table III with an underlined mark. It is also observed that the JMA intensity shows the lowest correlation (Table III) with PGV. Midorikawa *et al.* [14] pointed out that if long period contents are dominated in the records, correlation between the JMA intensity and PGV becomes bad. Since, some records used in this study contains long period motion, especially in the Chi–Chi earthquake records [29], the JMA intensity and PGV has rather low correlation. Note that the data points for the Chi–Chi earthquake are shown in Figures 3(c) and 3(d) with a plus sign.

Comparison of the results with liquefied records

The linear relationships between JMA intensity and PGA, PGV, and SI are derived for the liquefied records in this study as

$$I_{\text{JMA}} = 1.47 + 1.65 \log_{10} \text{PGA}_R \quad (\sigma = 0.200, R^2 = 0.778) \quad (28)$$

$$I_{\text{JMA}} = 2.64 + 1.64 \log_{10} \text{PGV}_R \quad (\sigma = 0.234, R^2 = 0.698) \quad (29)$$

$$I_{\text{JMA}} = 2.33 + 1.86 \log_{10} \text{SI} \quad (\sigma = 0.074, R^2 = 0.970) \quad (30)$$

For multiple ground motion indices, the linear relationships are derived as

$$I_{\text{JMA}} = 2.17 + 1.71 \log_{10} \text{SI} + 0.17 \log_{10} \text{PGA}_R \quad (\sigma = 0.074, R^2 = 0.971) \quad (31)$$

$$I_{\text{JMA}} = 1.44 + 0.78 \log_{10} \text{PGV}_R + 1.09 \log_{10} \text{PGA}_R \quad (\sigma = 0.172, R^2 = 0.848) \quad (32)$$

Note that although the liquefied records were selected from seven earthquake events, however, only one event contributed more than one record to this data set. Hence, the linear relationship

between JMA intensity and other ground motion indices for the liquefied records are derived performing a simple linear regression analysis.

Figure 8 shows the comparison of the relationships between I_{JMA} and PGA_{R} , PGV_{R} and SI , which are obtained from liquefied and non-liquefied records. One can see that the relationship between JMA intensity and PGA_{R} (Figure 8(a)) obtained from liquefied records shows higher intensity comparing to the one obtained from non-liquefied records. The common trend of liquefied site is that it has longer period, which may cause intensity to have higher value while estimating from PGA_{R} . However, with respect to both PGV_{R} and SI (Figures 8(b) and 8(c)), the relationships obtained from liquefied records show a large similarity with the ones obtained from the non-liquefied records. Midorikawa and Wakamatsu [16] calculated the intensities of the ground motion at liquefied sites during past earthquakes by semi-empirical method taking into account the fault size and the soil profile at the site. They concluded that PGV is better correlated with the occurrence of liquefaction than PGA and suggested that soil liquefaction is likely to occur when PGV exceeds 10–15 cm/s, which is supported by observation. Hence, for estimating the JMA intensity from liquefied records using single ground motion index, the choice of PGV_{R} or SI would be a better option than PGA_{R} . Figure 8(d) shows the comparison of the linear relationship between the JMA intensity estimated from liquefied and non-liquefied records using both SI and PGA_{R} . The relationship is obtained as

$$I_{\text{liq}} = 0.99I_{\text{non-liq}} \quad (33)$$

It means, in case of multiple ground motion indices, JMA seismic intensity estimated from liquefied records is only 1% lower in magnitude than the JMA seismic intensity estimated from non-liquefied records. Although it is observed that when JMA intensity is estimated from liquefied records using only PGA_{R} , it shows higher value than non-liquefied records, however, when it is estimated using both SI and PGA_{R} , the JMA intensity shows only 1 percent lower in magnitude than the non-liquefied records. It means, if JMA intensity is estimated using both SI and PGA_{R} , then SI dominates to the contribution of estimating the JMA intensity than PGA_{R} . Moreover, if we look at the all relationships (Equations (28)–(32)) obtained for the liquefied records, then it can also be seen that the JMA intensity shows the highest correlation ($R^2 = 0.971$) with the parameter such as the combination of both PGA_{R} and SI , and it shows the second highest correlation ($R^2 = 0.970$) with SI . The similar trend is also observed in case of the non-liquefied records.

Validity of the obtained relationships

As it is observed that JMA intensity shows the highest correlation with the parameter such as the combination of PGA and SI in the multivariate case and higher correlation with SI in the univariate case, it is also necessary to verify this observation, particularly, whether the JMA intensity shows the highest correlation with the combination of PGA and SI or not. In order to do so, we have selected 204 records from the 2000 Tottori-ken Seibu earthquake, which is not used in this study in the regression analysis for obtaining the relationship between JMA intensity and other ground motion parameters. Note that the magnitude (M_{W}) for the Tottori earthquake is 6.7. This magnitude is used in Equations (16) and (19) for the estimation of JMA intensity from SI and both SI and PGA for the selected 204 non-liquefied records of the Tottori earthquake. Figure 9 shows the relationship between the observed and estimated

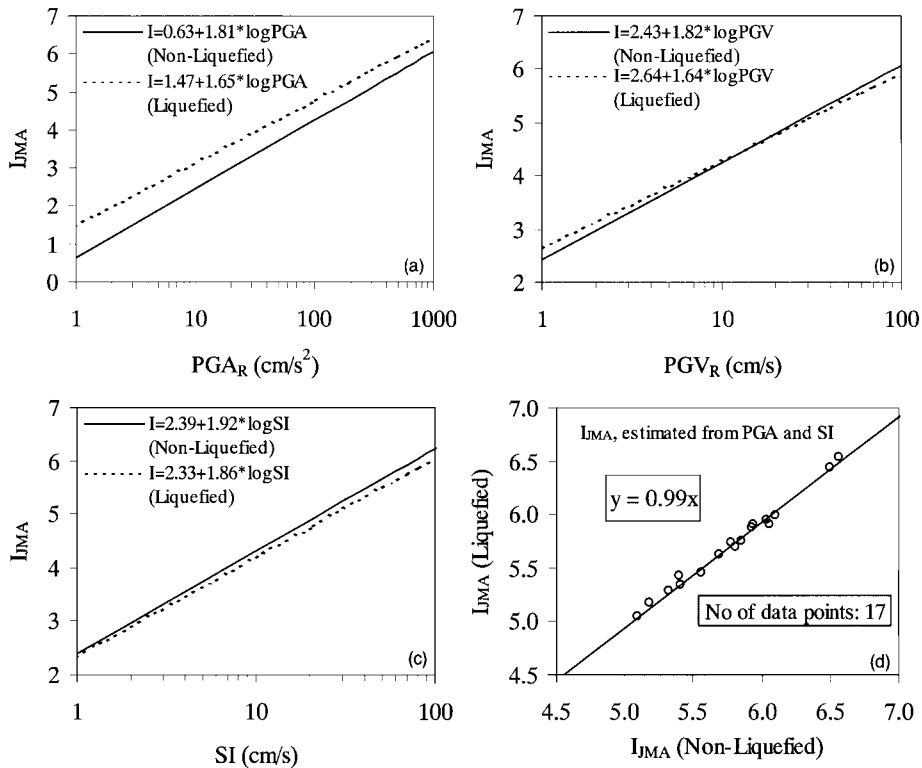


Figure 8. Comparison of the relationship between JMA intensity and ground motion indices obtained from the liquefied and non-liquefied records (a) with respect to PGA, (b) with respect to PGV, (c) with respect to SI, and (d) with respect to both PGA and SI.

JMA seismic intensity for 204 records of the Tottori earthquake. One can see that in the case JMA intensity is estimated from SI (Figure 9(a)), it shows only 1% lower value in magnitude than the observed one. On the other hand, in the case JMA intensity is estimated from the combination of SI and PGA (Figure 9(b)), it shows only 1% higher value in magnitude than the observed one. However, it can be seen that the correlation coefficient between observed vs estimated JMA intensity is higher in the case it is estimated from both SI and PGA ($R^2 = 0.980$) than only from SI ($R^2 = 0.932$). Moreover, one can also see that the data points of observed vs estimated JMA intensity shows less scattered in the case it is estimated from both PGA and SI than only from SI. This observation clearly indicates that the JMA seismic intensity shows the highest correlation with the combination of both PGA and SI.

CONCLUSIONS

The JMA seismic intensity and other ground motion indices, i.e., PGA, PGV, and spectrum intensity (SI) were calculated using two strong motion data sets; in which, the first set consists

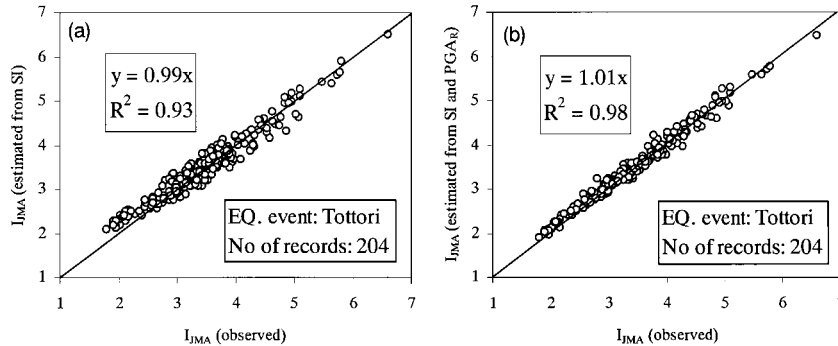


Figure 9. Relationship between the observed and estimated (in this study) JMA seismic intensity for the 204 non-liquefied records of the 2000 Tottori-ken Seibu earthquake.

of 879 non-liquefied records, and the second set consists of 17 liquefied records. The relationships between JMA intensity and PGA, PGV, and SI, were derived performing a two-stage linear regression analyses. The major findings are as follows:

1. The relationship between the JMA seismic intensity and strong motion parameters obtained in this study showed a very similarity with the ones obtained by Tong and Yamazaki and Midorikawa *et al.* with respect to both PGA and SI, however, some difference was observed with respect to PGV.
2. In case of single ground motion parameter, Midorikawa *et al.* concluded that JMA intensity shows higher correlation with PGV than PGA. However, in this study, it was observed that it shows higher correlation with SI than PGA or PGV. Moreover, it was also observed that JMA intensity shows higher correlation with PGA than PGV.
3. The relationship between JMA intensity and other ground motion parameters such as the product of PGA and PGV shows a very similarity comparing to the one obtained by Midorikawa *et al.*, however, in this study, it was observed that the JMA intensity shows higher correlation with the product of PGA and SI than the product of PGA and PGV.
4. In case of multiple ground motion parameters, very good agreement was observed between the relationship obtained in this study comparing to the one obtained by Tong and Yamazaki, and the JMA intensity shows the highest correlation with the parameters such as the combination of PGA and SI than the combination of PGA and PGV.
5. Comparing the correlation coefficients between the JMA intensity with all strong motion parameters, it follows as: (a) the JMA intensity shows the highest correlation with the parameters such as the combination of PGA and SI, (b) it shows the second highest correlation with the parameters such as the product of PGA and SI, and (c) it shows the next higher correlation with SI.
6. It was observed that the relationship between the JMA seismic intensity and strong motion parameters obtained from liquefied records showed a very similarity with the ones obtained from non-liquefied records with respect to both PGV and SI, however, some difference was observed with respect to PGA.

7. From the obtained relationship between the observed vs. estimated JMA intensity, it was found that the JMA intensity shows the highest correlation with the combination of PGA and SI than other strong motion parameters.

In case of implementation, according to the above findings, it can be concluded that for estimating the JMA seismic intensity from strong motion parameters, the choice of multiple ground motion parameters would be a better option rather than single ground motion parameter. The obtained relationships may be very useful for the disaster management agencies in Japan and deployment of new SI-sensors, which monitor both SI and PGA.

ACKNOWLEDGEMENTS

The authors express their sincere gratitude to Prof. M. Kikuchi from Earthquake Research Institute of the University of Tokyo, who kindly helped for checking the magnitude (M_W) for the all earthquake events provided by many organizations. All organizations, institutes, and private companies in Japan, the USA, and Taiwan mentioned in 'Earthquake Data' section that provided the strong motion records used in this study are also greatly acknowledged.

REFERENCES

1. Earthquake Research Committee. Seismic activity in Japan-Regional perspectives on the characteristics of destructive earthquakes-(excerpt). <http://www.hp1039.jishin.go.jp/eqchren/eqchrfrm.htm>, 1998.
2. Japan Meteorological Agency (JMA) Shindo wo Shiru (Note on the JMA seismic intensity). *Gyosei* 1996; 46–224 (in Japanese).
3. Shabestari KT, Yamazaki F. Attenuation relationship of JMA seismic intensity using JMA records. *Proceedings of the 10th Japan Earthquake Engineering Symposium*, vol. 1, 1998; 529–534.
4. Yamazaki F. Earthquake monitoring and real-time damage assessment systems in Japan-developments and future directions. *Proceedings of the 6th U.S.—Japan Workshop on Earthquake Resistant Design of Lifeline Facilities and Countermeasures Against Soil Liquefaction, Technical Report NCEER-960012*, 1996; 727–740.
5. Yamazaki F, Noda S, Meguro K. Developments of early earthquake damage assessment systems in Japan. *Proceedings of ICOSSAR'97, Structural Safety and Reliability*, 1998; 1573–1580.
6. Tong H, Yamazaki F. A relationship between seismic ground motion severity and house damage ratio. *Proceedings of the 4th US Conference on Lifeline Earthquake Engineering*, ASCE, 1995; 33–40.
7. Katayama T, Sato N, Saito K. SI-sensor for the identification of destructive earthquake ground motion. *Proceedings of the 9th World Conference on Earthquake Engineering*, vol. 7, 1988; 667–672.
8. Shimizu Y, Ishida E, Isoyama R, Koganemaru K, Nakayama W, Yamazaki F. Development of super high-density realtime disaster mitigation system for gas supply system. *Proceedings of the 6th International Conference on Seismic Zonation*, vol. 2, 2000; 1181–1186.
9. Shimizu Y, Watanabe A, Koganemaru K, Nakayama W, Yamazaki F. Super high density real-time disaster mitigation system. *12th World Conference on Earthquake Engineering*, CD-ROM, 2000; 7.
10. Yamazaki F, Shimizu Y. Super dense real-time monitoring of earthquakes for a city gas network in Japan. *Proceedings of the 17th International Symposium on Automation and Robotics in Construction*, 2000; 581–586.
11. Shimizu Y, Koganemaru K, Yamazaki F, Tamura I, Suetomi I. Seismic motion observed in Taipei basin by new SI sensors and its implication to seismic zoning. *Proceedings of the 6th International Conference on Seismic Zonation*, vol. 2, 2000; 497–502.
12. Midorikawa S. The correlation of the Japan meteorological agency intensity scale with physical parameters of strong ground motions. *Proceedings of the 7th European Conference on Earthquake Engineering*, vol. 2, 1982; 103–110.
13. Midorikawa S, Fukuoka T. Correlation of Japan meteorological agency intensity scale with physical parameters of earthquake ground motion. *Zishin* 1988; **41**(2):223–233 (in Japanese).
14. Midorikawa S, Fujimoto K, Muramatsu I. Correlation of New J.M.A. instrumental seismic intensity with former J.M.A. seismic intensity and ground motion parameters. *Journal of Social Safety Science* 1999; **1**:51–56 (in Japanese).

15. Tong H, Yamazaki F. Relationship between ground motion indices and new JMA seismic intensity. *Seisan-Kenkyu* 1996; **48**(11):65–68 (in Japanese).
16. Midorikawa S, Wakamatsu K. Intensity of earthquake motion at liquefied sites. *Soils and Foundations* 1988; **28**(2):73–84.
17. Kostadinov MV, Yamazaki F. Detection of soil liquefaction from strong motion records. *Earthquake Engineering and Structural Dynamics* 2001; **30**:173–193.
18. National Oceanic and Atmospheric Administration. *Earthquake Strong Motion CD-ROM*, National Geophysical Data Center, Boulder, 1996.
19. Central Weather Bureau. *Free-Field Strong Ground Data CD-ROM*, Seismological Center, Taiwan, 1999.
20. Fukushima Y, Tanaka T. A new attenuation relation for peak horizontal acceleration of strong earthquake ground motion in Japan. *Bulletin of the Seismological Society America* 1990; **80**(4):757–783.
21. Ambraseys NN, Bommer JJ. The attenuation of ground accelerations in Europe. *Earthquake Engineering & Structural Dynamics* 1991; **20**:1179–1202.
22. Boore DM, Joyner WB. The empirical prediction of ground motion. *Bulletin of the Seismological Society of America* 1982; **72**(6):S43–S60.
23. Joyner WB, Boore DM. Peak horizontal acceleration and velocity from strong-motion records including records from the 1979 Imperial Valley, California Earthquake. *Bulletin of the Seismological Society of America* 1981; **71**(6):2011–2038.
24. Molas GL, Yamazaki F. Attenuation of earthquake ground motion in Japan including deep focus events. *Bulletin of the Seismological Society of America* 1995; **85**(5):1343–1358.
25. Neter J, Wasserman W, Kutner MH. *Applied Linear Regression Models* (2nd edn). IRWIN: Boston, 1989.
26. Draper N, Smith H. *Applied Regression Analysis* (2nd edn), Wiley: New York, 1981.
27. Kawashima K, Aizawa K, Takahashi K. Effects of composition of two horizontal components on attenuation of maximum earthquake ground motions and response spectra. *Proceedings of the Japan Society of Civil Engineers*, 1983; **329**:49–56 (in Japanese).
28. Ansary MA, Yamazaki F, Katayama T. Statistical analysis of peaks and directivity of earthquake ground motion. *Earthquake Engineering and Structural Dynamics* 1995; **24**:1527–1539.
29. Loh C-H, Lee Z-K, Wu T-C, Peng S-Y. Ground motion characteristics of the Chi-Chi earthquake of 21 September 1999. *Earthquake Engineering and Structural Dynamics* 2000; **29**:867–897.
30. Aki K. Generation and propagation of *G* waves from the Niigata earthquake of June 16, 1964. Part 2. Estimation of earthquake moment, release of energy, and stress–strain drop from *G* wave spectrum. *Bulletin of the Earthquake Research Institute* 1966; **44**:73–88.